

aluminum alloys. The following sections present some of these studies on laminated DRA materials. In particular, the fracture resistance of DRA laminates is compared to that of monolithic DRA materials. Additionally, mechanisms for the improvement of crack stability in DRA laminates are reviewed.

Survey of DRA Laminates

As shown in Figure 1, there are two manners in which a laminate may be loaded: the crack arrestor orientation and the crack divider orientation. In the crack arrestor orientation, crack growth proceeds normal to the interface between the laminae. By contrast, crack growth in the crack divider orientation occurs parallel to the bondplane between the constituents. Fracture resistance of DRA laminates may be determined under static or dynamic loading conditions. In the case of DRA laminate plate product under Mode I loading, the fracture resistance in the crack divider and crack arrestor orientations may be tested, although the crack divider toughness may be more critical. By contrast, impact damage in a DRA laminate plate product is most probable in the crack arrestor orientation.

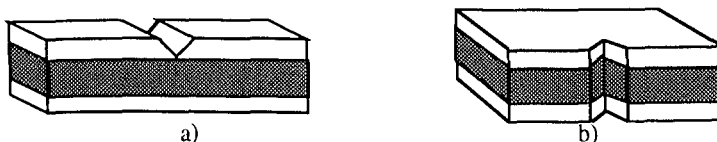


Figure 1. a) The crack arrestor orientation and b) the crack divider orientation.

The DRA laminate systems which have been investigated have ranged from two layers to over 20 layers and have been processed via hot pressing[10-12,15-18], co-extrusion[2,10-12] roll bonding[5,13], or adhesive bonding[4,5,9,13,25] techniques. While the materials, the number of layers, and the processing routes may vary between DRA laminates, common trends have begun to develop in the fracture resistance of DRA materials. The purpose of this section is to first survey the DRA laminate systems which have been studied and then present the observations of enhanced fracture resistance provided by a laminate structure.

DRA Laminate Systems

Table I lists the DRA laminate systems which are considered in this paper. The fracture resistance of these laminates have been tested in various manners. The 6090/SiC/25p-5182 system has predominantly been evaluated via the use of Chevron-notched three-point bend bars. By contrast, the MB85/SiC/15p-3003, MB85/SiC/15p-6061, 7093/SiC/15p-7093, and X2080/SiC/20p-X2080 systems have been analyzed using machine-notched three-point bend and compact tension specimens (ASTM E399, E813, and E992) as well as instrumented Charpy impact testing (ASTM E23). While direct comparisons between the testing techniques may be difficult, consideration of all of the fracture toughness values obtained from these experiments leads to an improved understanding of the enhancement in fracture resistance prouced in DRA laminates.

Table I. DRA Laminate Systems

DRA (Number of Layers)	Al Alloy (Number of Layers)	Reference
MB85/SiC/15p (1)*	3003, 1100, or 6061(1)	[10-12]
7093/SiC/15p (1)	7093 (2)	[5,13]
6090/SiC/25p (up to 10)	5182 (up to 11)	[15-18]
X2080/SiC/20p (3)	X2080 (2)	[4,9,25]

* - MB85 is a P/M 2XXX alloy

DRA Laminate Fracture Resistance

Figure 2 displays the toughness values for the 6090/SiC/25p-5182 system as determined by Chevron-notched bend specimens. The laminated structures represent a marked improvement in the fracture resistance over that of an unlaminated DRA material. Additionally, the laminates tested in the crack arrestor orientation displayed a slightly greater fracture toughness over that of those tested in the crack divider orientation, although in other studies, the difference in toughness has been greater. The important factor from Figure 2 is the retention of enhanced fracture resistance even when approaching 97% DRA (*i.e.*, DRA layers comprise 97% of the laminate).

These tests illustrate the ability of DRA laminates to dramatically increase the fracture toughness of DRA materials. The enhancement in fracture resistance can be further seen by analyzing DRA laminates under conventional ASTM procedures. These testing methods allow for the separation of toughness improvement into fracture initiation and crack growth resistance. An monolithic DRA material exhibits approximately linear behavior under three-point bending as shown in Figure 3. By contrast, the DRA laminate shown in Figure 3 displays an increased maximum load and bend ductility, both contributing to a marked improvement in Mode I fracture resistance as shown in Table II.[13]

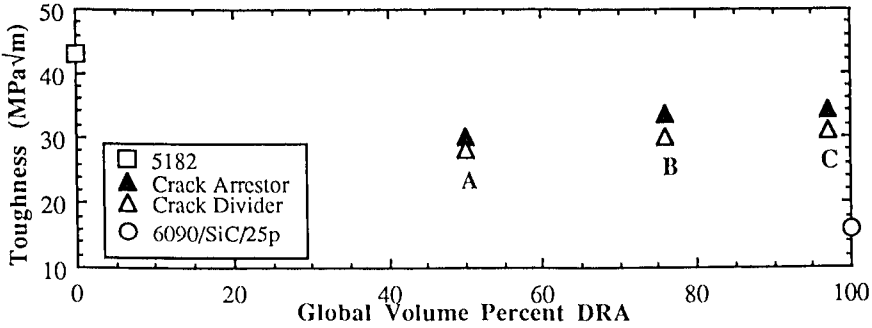


Figure 2. Toughness (from Chevron notched specimens) for the 6090/SiC/25p-5182 system (T6 condition). [A = 0.6 mm DRA layer, B = 1.3 mm DRA layer, and C = 2.0 mm DRA layer]

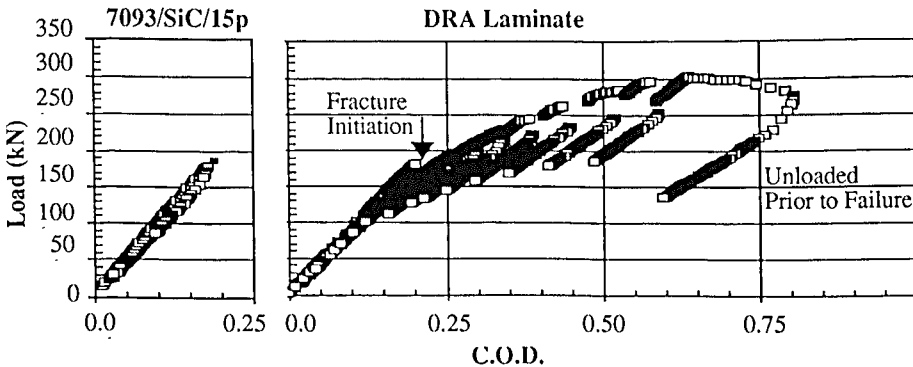


Figure 3. Comparison of the load versus crack opening displacement curves for 7093/SiC/15p-T7E92 and a roll bonded tri-layer DRA laminate [two layers of 7093-T7E92 (2.5 mm each) and one layer of 7093/SiC/15p-T7E92 (5.0 mm)]

Table II. Crack divider toughness.

Material	Toughness Values*	Type of Test
MB85/SiC/15p-UA	$J_{IC} = 8 \text{ kJ/m}^2$ $T = 0.9^{**}$	Compact tension
Press bonded bi-layer laminate (MB85/SiC/15p-6061)	$J_{IC} = 9 \text{ kJ/m}^2$ $T = 2.5^{**}$	Compact tension
7093-T7E92	$KQ = 42.2$ $K_{EE} = 42.2$ $\text{MPa}\sqrt{\text{m}}^{***}$	Three-point bend
7093/SiC/15p-T7E92	$KQ = 23.3$ $K_{EE} = 23.3$ $\text{MPa}\sqrt{\text{m}}^{***}$	Three-point bend
Roll bonded tri-layer laminate	$KQ = 21.0$ $K_{EE} = 41.1$ $\text{MPa}\sqrt{\text{m}}^{***}$	Three-point bend
Adhesively bonded tri-layer laminate	$KQ = 19.0$ $K_{EE} = 34.0$ $\text{MPa}\sqrt{\text{m}}^{***}$	Three-point bend
X2080/SiC/20p-T6	$KQ = 26.0$ $K_{EE} = 26.0$ $\text{MPa}\sqrt{\text{m}}^{***}$	Three-point bend
Adhesively bonded 5-layer laminate (2.7 mm layers)	$KQ = 23.1$ $K_{EE} = 34.0$ $\text{MPa}\sqrt{\text{m}}^{***}$	Three-point bend
Adhesively bonded 5-layer laminate (2.0 mm layers)	$KQ = 24.4$ $K_{EE} = 38.6$ $\text{MPa}\sqrt{\text{m}}^{***}$	Three-point bend

* - KQ is determined based upon ASTM E399, J_{IC} is determined based upon ASTM E813, K_{EE} is determined based upon ASTM E992, and T is the tearing modulus.

** - Crack extension was monitored on the DRA surface.

*** - Extensive non-planar crack growth invalidated a J-integral approach; therefore, ASTM E992 was adopted as a means to quantify crack growth resistance.[9,13]

Table III. Crack arrestor impact resistance

Material	DRA thickness (mm)	Al thickness (mm)	Energy absorbed (J/cm ²)
MB85 - UA	-	10	28.3
MB85/SiC/15p - UA	10	-	3.2
Press bonded laminate	7.2	2.8	40.4
Press bonded laminate	6.0	4.0	56.0
7093-T7E92	-	10	8.2
7093/SiC/15p-T7E92	10	-	2.0
Roll bonded laminate	5.0	2.5 (two layers)	28.4
Adhesively bonded laminate	5.0	2.5 (two layers)	9.5

As mentioned earlier, the impact resistance in the crack arrestor orientation may be critical for DRA laminate plate product. As shown in Table III, DRA laminates represent a great improvement in impact resistance over that of unlaminated DRA materials. As in the case of the crack divider toughness, the level of enhancement may be affected by the processing route, the alloy composition, and the interfacial characteristics. In order to better understand the method by which laminates improve the fracture resistance of DRA materials as well as to rationalize the influence of laminate construction on toughness, the fracture mechanisms in these materials must be considered. The following section, therefore, details the fracture processes and the relationships between crack growth and fracture resistance in DRA laminates.

Fracture Processes in DRA Laminates

One of the driving forces behind in the investigation of laminated structures consisting solely of monolithic materials is the increased toughness of sheet material due to a transition from plane strain to plane stress conditions.[20,22,26] In the case of DRA laminates, great improvements in DRA toughness may be achieved even when the thickness of the DRA layers is greater than the critical thickness for the transition to plane stress behavior. In the 6090/SiC/25p-5182 system, a shear fracture mode was observed in 6090/SiC/25p which would exhibit a plane strain, flat fracture surface if tested alone.[18] Similarly, stable crack growth has been observed in DRA layers which would otherwise fracture without any crack growth resistance.[9-14] In order to rationalize the crack stability in DRA laminates, the crack growth mechanisms need to be considered. Figure 4 displays the fracture surfaces for 6090/SiC/25p-5182 laminates tested in the crack arrestor and the crack divider orientations. There is evidence of an extremely tortuous crack path as well as increased energy absorption due to interfacial delamination and plastic deformation of the aluminum layers. A better understanding of the fracture mechanisms in both orientations has been gathered via in-situ monitoring of crack growth as well as serial sectioning of specimens unloaded prior to failure.[13,14]

In the crack arrestor orientation, three-point bend specimens have been tested to determine the crack growth mechanisms in both impact loading as well as bending at slower strain rates.[5,13,25] As shown in Figure 5, crack growth in the crack arrestor orientation is much different than that in a monolithic material. Fracture in a monolithic DRA material is concentrated in a localized region and a planar fracture surface is produced. By contrast, extensive non-planar crack growth and crack blunting can occur in the crack arrestor orientation via interfacial delamination or plastic deformation of the unreinforced aluminum layer. As a result, crack arrest is produced in which continued propagation can only occur after re-initiation on the tensile surface of subsequent layers in a manner analogous to an unnotched bend bar.

In the crack divider orientation, preferential initiation can occur in the DRA layers. Although some improvement in initiation resistance has been found in the MB85/SiC/15p-1100 system[10], a greater increase in toughness is seen in the resistance to crack growth. Once again, this is directly related to the crack propagation mechanism as shown in Figure 6. Cracking can in the DRA layer can be stabilized via a crack bridging mechanism.[14] The uncracked aluminum ligaments in the crack wake retard crack propagation in the DRA layers. Additionally, DRA crack growth can be further retarded if controlled interfacial delamination occurs.[13] Interfacial delamination increases the area in which fracture related events occurs as well as inducing mixed mode loading.

Finally, differences in the fracture behavior of DRA laminates may also be explained by considering the fracture mechanisms. The intrinsic fracture resistance of the DRA material will affect the toughness of the DRA laminate. This can be seen in the X2080/SiC/20p-X2080 system by a comparison of the laminates with 2.7 mm and 2.0 mm layers.[9] The superior fracture resistance of the laminate containing 2.0 mm layers may be in part due to the improved intrinsic fracture toughness of the 2.0 mm X2080/SiC/20p layers. Similarly, the greater impact resistance in the MB85/SiC/15p-3003 system when compared to the 7093/SiC/15p-7093 system in Table III may be related to the greater inherent impact resistance of the 2XXX-based material when compared to the 7XXX-based material.

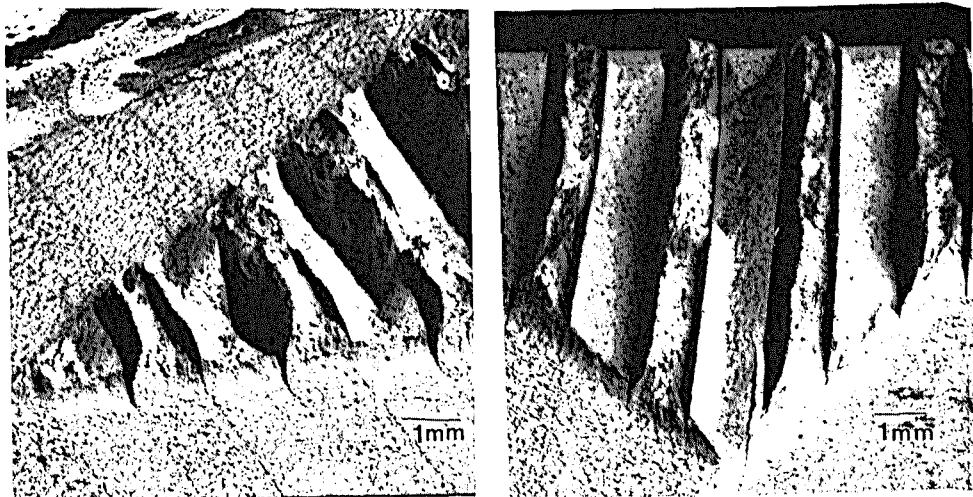
The behavior of the interfacial regions will also influence the fracture of DRA laminates. As stated above, the predominate energy absorption mechanisms in DRA laminates may be crack bridging and controlled interfacial delamination. To a first approximation, fracture resistance scales directly with the length of delamination. The lower fracture toughness of the adhesively bonded 7093/SiC/15p-7093 laminate in Table II when compared to the roll bonded 7093/SiC/15p-7093 laminate may be related to the lack of interfacial delamination. While crack growth in adhesively bonded laminates may be retarded via bridging by the aluminum layer[9,13,25], greater crack extension occurs with lower energy absorption due to the lack of interfacial delamination.

Conclusion

DRA laminates represent a marked improvement in fracture resistance over monolithic DRA materials. This improvement is directly related to the fracture mechanisms which operate in laminated structures. Extensive non-planar crack propagation can be produced via crack bridging by the monolithic aluminum layers and through controlled interfacial delamination. As a result, stable crack growth and an increased fracture resistance are produced in a DRA material.

Acknowledgements

The authors would like to acknowledge the support and permission to publish from Alcoa, Lawrence Livermore National Laboratory, NSF-DMR-PYI-89-58326 (JL,TMO), ARO-DAL03-89-K0068 (JL,TMO).



a) b)
Figure 4. Fracture surfaces for the 6090/SiC/25p-5182 system tested in a) the crack arrestor orientation and b) the crack divider orientation [Chevron-notched three-point bend bars]. Note the plastic stretch in the unreinforced aluminum layers as well as delamination between the layers.

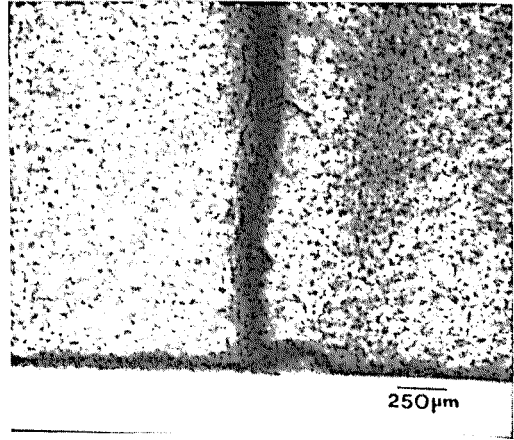
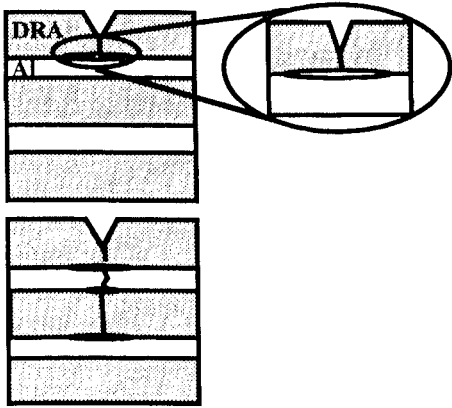


Figure 5. a) Schematic of crack arrester crack growth and b) crack arrest via interfacial delamination after growth through a DRA layer in the crack arrester orientation [7093/SiC/15p-7093 system]

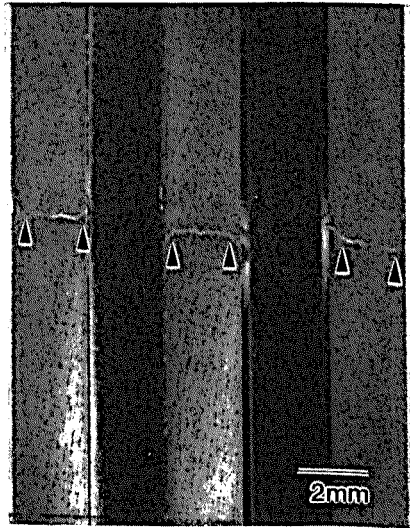
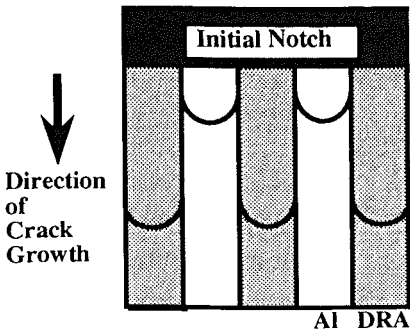


Figure 6. a) Schematic of crack divider crack growth and b) near crack tip region in an adhesively bonded five-layer laminate [X2080/SiC/20p-T6 (three layers, 2.0 mm each) and X2080-T6 (two layers, 2.0 mm each)] tested in the crack divider orientation.

References

1. D.L. McDaniels, Metall. Trans. A 16A, (1985), 1105.
2. J.J. Lewandowski, C.Liu, W.H.Hunt, Jr., Mat. Sci. Eng A107, (1989), 241.
3. S.V. Kamat, J.P. Hirth, and R. Mehrabian, Acta Metall. **37**, (1989), 2395.
4. T.M. Osman, J.J. Lewandowski, and W.H. Hunt, Jr., Advances in Powder Metallurgy and Particulate Materials-1994, (Princeton NJ, USA: Metal Powder Industries Federation, 1994), in press.
5. W.H. Hunt, Jr., T.M. Osman, and J.J. Lewandowski, JOM **45**, (January 1993), 30.
6. M. Manoharan and J.J. Lewandowski, Acta Metall. **38**, (1990), 489.
7. M. Manoharan and S.V. Kamat, J. Mat. Sci. **28**, (1993), 5218.
8. R.D. Goolsby and L.K. Austin, ICF-7. Advances in Fracture Research, (1989), p. 2423.
9. T.M. Osman and J.J. Lewandowski, Scripta Metall., (1994), in press.
10. M. Manoharan, L. Ellis, and J.J. Lewandowski, Scripta Metall. **24**, (1990), 1515.
11. L. Yost Ellis and J.J. Lewandowski, J. Mat. Sci. Letters **10**, (1991), 461.
12. L. Yost Ellis and J.J. Lewandowski, Mat. Sci. Eng., (1994), in press.
13. T.M. Osman, J.J. Lewandowski, and W.H. Hunt, Jr., Metall. Trans. A, in review.
14. T.M. Osman, P.M. Singh, and J.J. Lewandowski, Scripta Metall., in press.
15. C.K. Syn, et al., Developments in Ceramic and Metal-Matrix Composites, ed. K. Upadhyya (Warrendale, PA, USA: TMS, 1992), 311.
16. C.K. Syn, D.R. Lesuer, and O.D. Sherby, Advanced Synthesis of Engineered Structural Materials, eds. J.J. More, E.J. Lavernia, and F.H. Froes, (Materials Park, OH, USA: ASM International), 149.
17. C.K. Syn, D.R. Lesuer, and O.D. Sherby, Light Materials for Transportation Systems, ed. N.J. Kim, (Kyongju, Korea: 1993), 763.
18. C.K. Syn, S. Stoner, D.R. Lesuer, and O.D. Sherby, High Performance Ceramic and Metal Matrix Composites, (Warrendale, PA, USA: TMS, 1994), p. 125.
19. R.O. Ritchie, Mat. Sci. Eng. A103, (1988), 15.
20. J. Kaufman, J. of Basic Engineering, (1967), 503.
21. E.A. Almond, J.D. Embury, and E.S. Wright, Trans. of the Metallurgical Society of AIME **239**, (1967), 114.
22. R.D. Goolsby, Int. Conf. on Composite Materials, (Warrendale, PA, USA: TMS, 1971), 941.
23. Y. Oshai, J. Wolfenstine, R. Koch, and O.D. Sherby, Mat. Sci. Eng. A151, (1992), 37.
24. C.K. Syn, D.R. Lesuer, and O.D. Sherby, Metall. Trans. A 24A, (1993), 1647.
25. T.M. Osman, W. Gerhart, and J.J. Lewandowski, in preparation.
26. J.F. Knott, Fundamentals of Fracture Mechanics, (London, UK: Edward-Arnold, 1986).